FORECAST SENSITIVITY OF LAKE-EFFECT SNOW TO CHOICE OF BOUNDARY LAYER PARAMETERIZATION SCHEME

Robert Conrick[1,2] and Heather Reeves[3]

[1]National Weather Center Research Experiences for Undergraduates Program
Norman, Oklahoma
[2]Indiana University, Bloomington, Indiana

[3]Oklahoma University Cooperative Institute for Mesoscale Meteorological Studies & NOAA National Severe Storms Laboratory, Norman, Oklahoma

ABSTRACT

This study assesses the forecast sensitivity of lake-effect snow to various boundary layer parameterization schemes using the WRF-ARW model. Six boundary layer schemes are tested on a case-study of lake-effect snow over Lake Erie in Dec 2009. The experiments reveal significant precipitation differences (as much as 20 mm over 6 h) between the schemes. Consideration of the heat and moisture fluxes shows that schemes producing more precipitation have higher fluxes over the lake. Forcing all schemes to use the same over-water heat and moisture fluxes causes the precipitation forecasts to be in closer agreement. The heat and moisture fluxes are found to be strongly dependent on the similarity-stability functions for heat, momentum, and moisture (Ψ_H, Ψ_M, and Ψ_Q). When the over-water values for Ψ_H, Ψ_M, and Ψ_Q are set to be the same in all schemes, precipitation forecasts are similar in all experiments, thus indicating that the parameterization used to determine Ψ_H, Ψ_M, and Ψ_Q can have profound impacts on forecasts of this type of weather. Comparison of the forecast accumulated precipitation to observations shows that most schemes over predict the precipitation. The scheme in closest agreement is the Mellor-Yamada-Nakanishi-Niino scheme.

1. INTRODUCTION

The accurate prediction of lake-effect snow (LESN) is a challenge for the Great Lakes region of North America. These storms have significant impacts on communities around the Great Lakes not only because they can produce copious amounts of snow, but also because the snow bands are quite narrow (ranging from 10 to 50 km), which makes their prediction especially challenging. LESN is also difficult to predict because the clouds are confined to the boundary layer, implying that numerical weather forecasts of these storms may be vulnerable to the assumptions and biases inherent in certain boundary layer parameterization schemes. In this study, the sensitivity of numerical weather forecasts of LESN to the choice of boundary layer parameterization is tested.

There are three primary categories of LESN. These are single along-shore or midlake bands, multibanded or widespread banding, and mesoscale vorticies (e.g., Kelly 1982; Peace and Sykes 1966; Forbes and Merrit 1984). The category of band is dictated by the ratio of low-level wind speed to the fetch of the lake (Laird et al. 2003). Because operational numerical weather prediction (NWP) models were not capable of resolving individual LESN bands until recently, forecasters historically have used an ingredients-based methodology to both anticipate LESN type and amount. These ingredients include the temperature difference between the lake and 850mb, the wind direction from the boundary-

[1] *Corresponding author address:*
Robert Conrick, Department of Geography, Indiana University Bloomington.
119 W. Michigan Ave., Chesterton, IN 46304
rconrick@indiana.edu

layer through 700 mb, the change in wind direction with height, and the presence and height of the low-level inversion (Niziol 1987). However, recent advances in computing capabilities both at the national scale and within individual forecast offices allow for high-resolution forecasts [O(1-4 km)] that are capable of resolving individual bands. It is hoped that this will allow for more precise forecasts of precipitation amounts.

Relatively little work has been done to understand constraints and limitations of .high-resolution NWP of LESN. Some studies have addressed how altering the microphysical parameterization scheme affects LESN forecasts (Reeves and Dawson 2012). The effects assimilating certain observations (Scott and Sousounis 2001; Zhao et al. 2012) and the effects of ice coverage (Vavrus et al. 2013; Wright et al. 2013) have also received limited attention. But, to the best of our knowledge there has been no investigation into the sensitivity to boundary layer parameterization scheme. Given that LESN cloud systems are completely contained within the boundary layer, it is reasonable to suspect some sensitivities may exist.

The aim of this study is to assess whether NWP forecasts of LESN are sensitive to the choice of boundary layer parameterization and if so, why. This is done through a series of numerical model sensitivity experiments of a select event of LESN. This paper is organized as follows. The case study and numerical experiment design are described in Section 2. Results of the experiments are described in Section 3. Model validation is presented in Section 4. Concluding thoughts are provided in Section 5.

2. DATA AND METHODOLOGY

a. Case study: Dec. 10-12, 2009

For this study, a particularly strong LESN event that occurs between 10 and 12 Dec 2009 over Lake Erie is used. The observed composite reflectivity at 2200 UTC 10 Dec, during the time when the band is most intense, shows that this is a single-banded form that is adjacent to the east coast of Lake Erie and extends over the greater Buffalo area (Fig. 1a). At this time, the low-level wind is from the west-southwest and there is a weak trough/ridge pairing collocated with the band. A vertical cross section of observed reflectivity parallel to the low-level wind direction shows that as the air encounters the east shore of the lake and the moderate topography of western New York, the convection is greatly enhanced (Fig. 1b). The equivalent potential temperature contours show that most of the convection is contained within the surface-based mixed layer, although some cloud turrets extend above this layer. The 24-h accumulated liquid equivalent precipitation estimate (Lin and Mitchell 2005) starting at 1200 UTC 10 Dec has dual maxima. The lesser (27.44 mm) is near Dunkirk, New York, along the east shore of Lake Erie (Fig. 2). The other (30.99 mm) is farther inland, east of Buffalo.

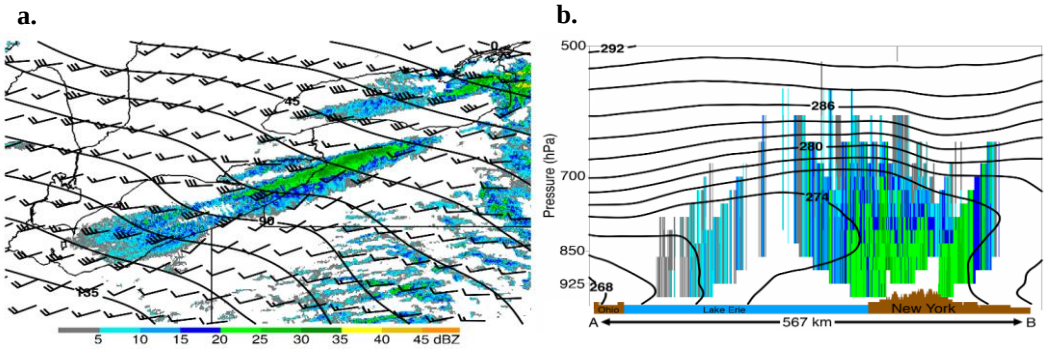

FIG. 1: 2200 UTC 10 Dec 2009 (a) Observed composite reflectivity (shaded), RUC-analyzed 10-m wind barbs and 1000-hPa heights (contoured) and (b) vertical cross section of composite reflectivity (shaded) and RUC-analyzed equivalent potential temperature (contoured).

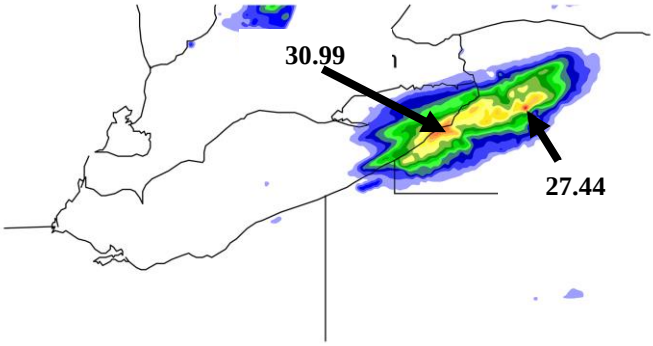

FIG. 2: Stage IV precipitation analysis for the case study in question. Arrows point to the maxima observed in this snow band.

b. Experiment Design

Experiments are conducted using the Advanced Weather Research and Forecasting (WRF-ARW) Model Version 3.5. The experiments are initialized at 0000 UTC 10 December 2009 and are integrated for 48 hours with a 12-second time step. The grid spacing is 4 km and there are 51 vertical levels. The domain has 200 grid points in both the x and y directions (Fig. 3). Parameterization schemes include the Noah land-surface model (Ek et al. 2003), the Thompson microphysical scheme (Thompson et al. 2004), and the Dudhia long- and shortwave radiation schemes (Dudhia 1989). The initial and boundary conditions are from the North American Mesoscale Model (NAM; Janjic et al. 2005) forecast initialized at 0000 UTC 10 December 2009. Six different planetary boundary-layer (PBL) parameterization schemes are considered. These are the BouLac (Bougeault and Lacarrere 1989), Mellor-Yamada-Janjic (MYJ; Janjic 2002), Mellor-Yamada-Nakanishi-Niino (MYNN2; Nakanishi and Niino 2004), Asymmetric Convective Model 2 (PX; Pleim 2007), Quasi-Normal Scale Elimination (QNSE; Sukoriansky et al. 2006), and Yonsei University (YSU; Hong et al. 2006). Each PBL scheme was paired with its corresponding surface-layer scheme, with the exception of BouLac, which has none within WRF and thus was paired with the MYJ surface-layer scheme.

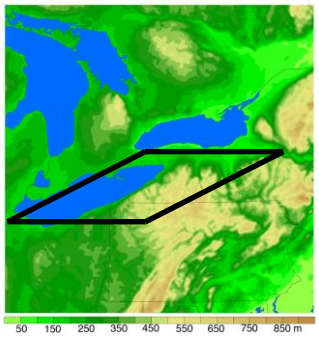

FIG.3 : The model domain used in this study, including terrain. The parallelogram denotes the area used for area integrated and area maximum precipitation analyses.

3. RESULTS

a. Control Runs

A set of six experiments are performed that are identical except for the choice of boundary layer parameterization. These are referred to as the control runs. Let us first consider the accumulated liquid-equivalent precipitation between 1800 and 2400 UTC 10 Dec. This is the period when all schemes produce the most precipitation. While all experiments place the band and maxima in similar locations, the magnitude of precipitation that falls varies widely among the schemes (Figure 4). The BouLac, MYJ, PX, and

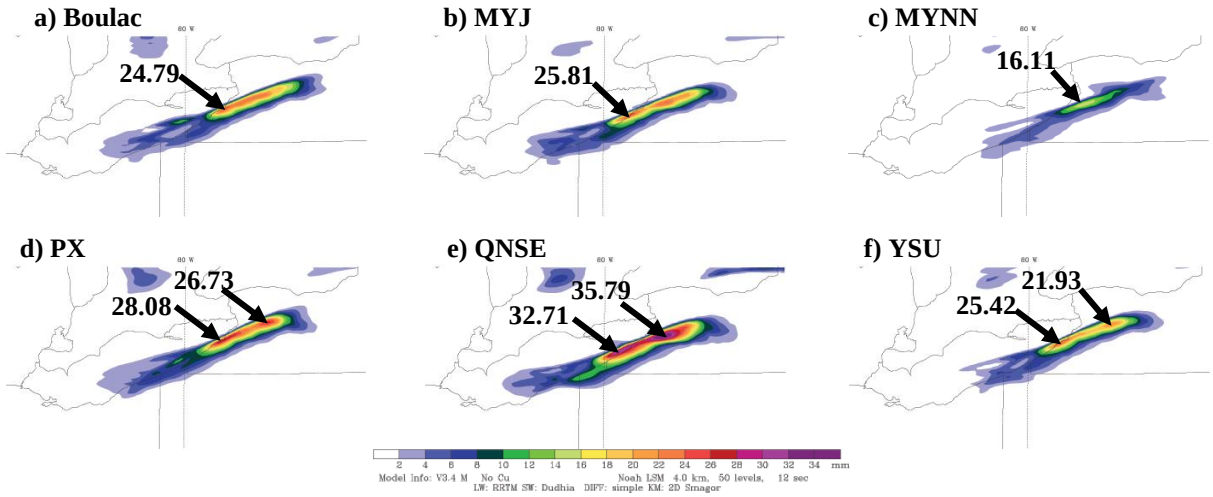

FIG. 4: 6-Hour Liquid-Equivalent Precipitation from 1800-2400 UTC December 10, 2009 for the control runs. Maxima locations and quantities are marked. Schemes Boulac (a), MYJ (b), PX (d), and YSU (f) have approximately equal quantities of precipitation, while scheme MYNN (c) has the least of the six control runs and scheme QNSE (e) has the most of the six control runs. Precipitation location is approximately equal for all schemes.

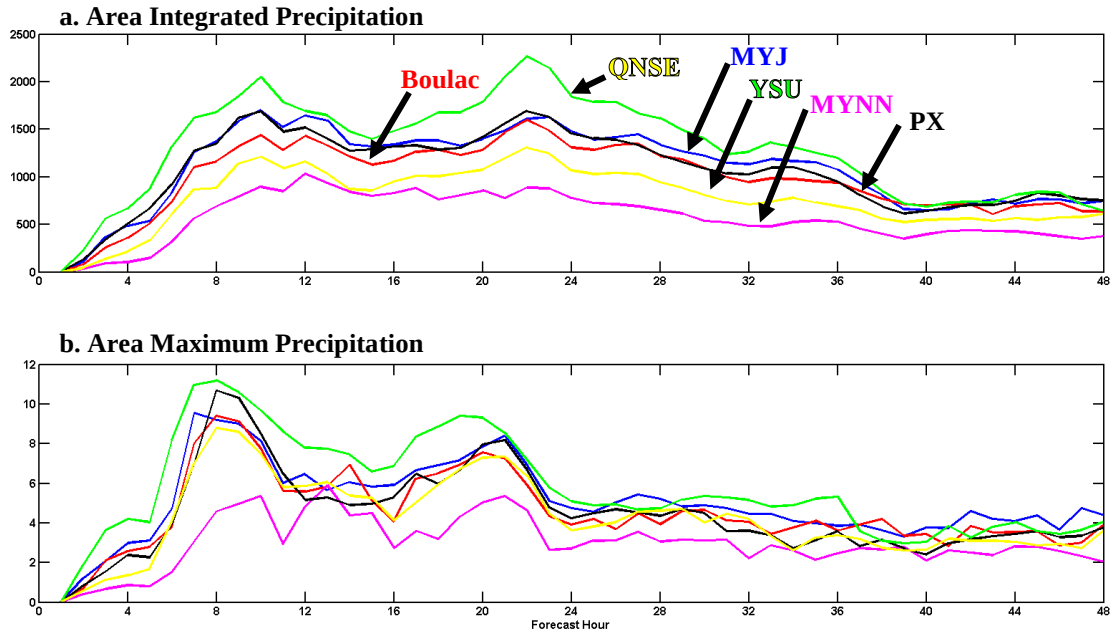

FIG. 5: Control run (a) area integrated precipitation and (b) area maximum precipitation for the six schemes tested. Note the significant differences in precipitation between schemes.

YSU experiments have maxima ranging from 24.79 mm to 28.08 mm (Figs. 4a,b,d,f). In contrast, MYNN and QNSE have maxima of 16.11 and 35.79 mm, respectively (Figs. 4c,e).

A time trend of precipitation is obtained by integrating the hourly precipitation at each grid point in the parallelogram shown in Fig. 3. In this analysis, QNSE has the highest precipitation and MYNN the lowest (Fig, 5a). All other schemes produce similar amounts of precipitation. One can also consider the hourly maximum within the parallelogram. As above, QNSE has comparatively high and MYNN comparatively low maxima (Fig. 5b).

It seems logical to presume that these differences in precipitation are the result of over-water modification of air parcels. To assess this, forward trajectories are started at the surface at 1800 UTC 10 Dec along the west coast of Lake Erie. These trajectories (shown only for QNSE, MYJ, and MYNN; Figs. 6a-c) indicate that the direction of the low-level flow is similar in all experiments. But, the air mass modification along these trajectories differs substantially in each experiment shown. QNSE (MYNN) is subject to greater (lesser) warming, acceleration, and moistening (Figs. 6d-f). Boulac, PX, and YSU are similar to MYJ (not shown). The increased warming and moistening in QNSE is of particular interest because either increases the potential for precipitation.

Deeper investigation reveals that the different warming and moistening may be due to differing heat and moisture fluxes (HFX and QFX). Boulac, MYJ, PX, and YSU have a similar HFX over Lake Erie (Figs. 7a,b,d,f). But QNSE (MYNN) has a relatively high (low) HFX (Figs. 7c,e). Similar differences exist in QFX (not shown).

b. Constant-Flux Experiments

To gauge whether the different heating and moistening is a consequence of the different HFX and QFX over Lake Erie, experiments are conducted wherein the over-water HFX and QFX are set 550 W m-2 and 165x10-6 kg m-2 s-1 respectively. These experiments are referred to as the constant-flux experiments.

The 6-hr accumulated precipitation for the constant-flux experiments shows closer agreement than in the control experiments (c.f. Figs.4,8). Maxima for the constant-flux BouLac, MYJ, PX, and YSU range from 22.14 mm to 25.44 mm (Figs. 8a,b,d,f). QNSE and MYNN – the outliers in the control runs – are now in closer agreement with the other schemes,

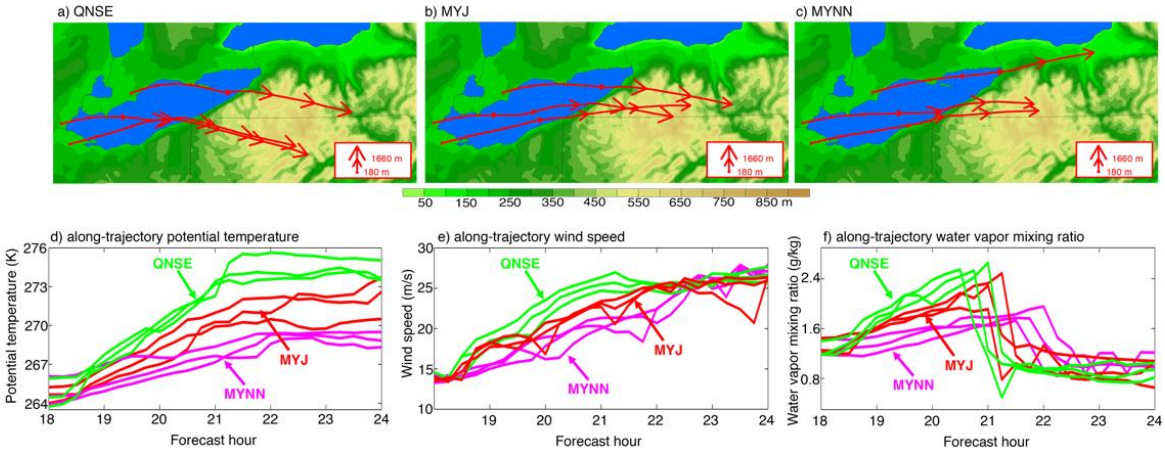

FIG. 6: Air parcel trajectory analysis for schemes QNSE, MYJ, and MYNN. The top panels show the paths that parcels took across Lake Erie. Bottom panels show how the parcels are modified as they traverse the lake. QNSE warms and moistens at a faster rate and to a greater quantity than MYNN.

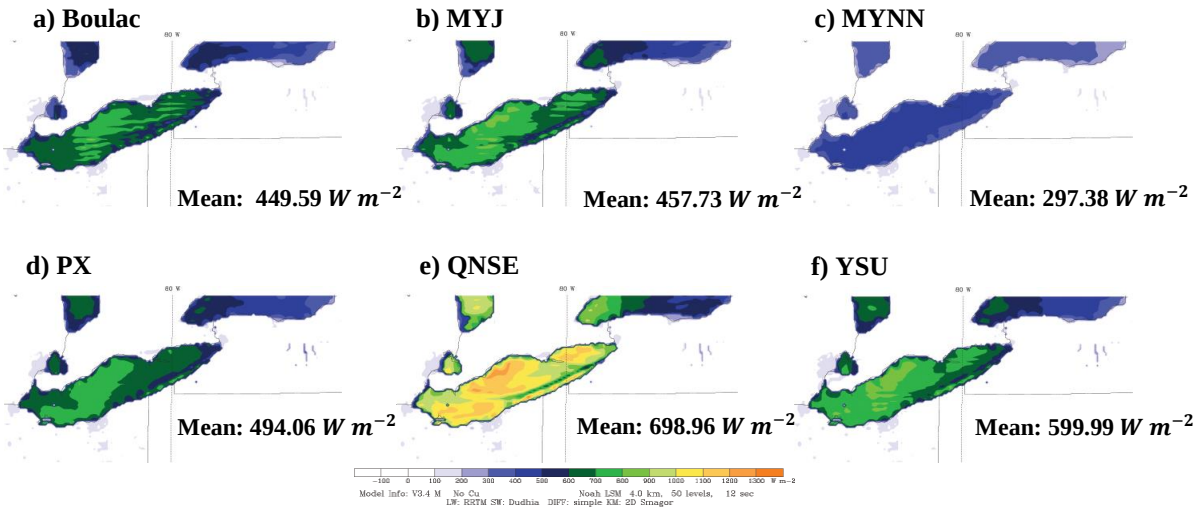

FIG. 7: Heat flux (HFX) on 2100 UTC December 10, 2009 for control runs over Lake Erie. Mean values are shown. As with figure 3, schemes Boulac (a), MYJ (b), PX (d), and YSU (f) have approximately equal mean HFX, while scheme MYNN (c) has the least of the six control runs and scheme QNSE (e) has the most of the six control runs.

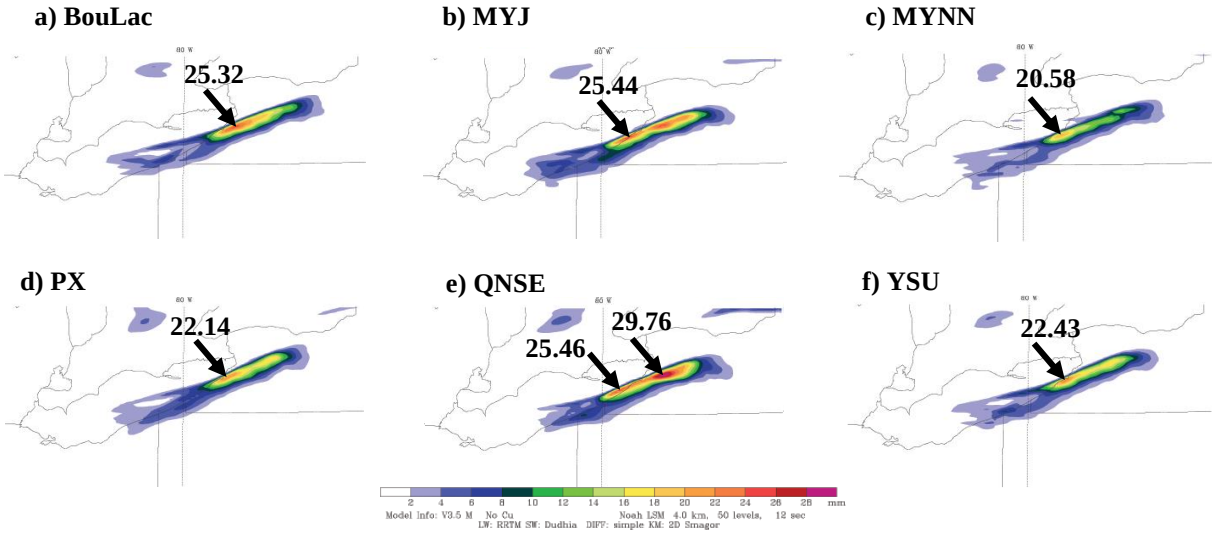

FIG. 8: 6-Hour Liquid-Equivalent Precipitation from 1800-2400 UTC December 10, 2009 for runs with constant heat flux (HFX=550 W/m2) and moisture flux (QFX=165E-6 kg/m2/s). Maxima locations and quantities are marked. The difference in precipitation between the maximum (QNSE; 29.76 mm) and the minimum value (MYNN; 20.58 mm) is approximately 10 mm, which is approximately half the difference exhibited in the control runs.

having maxima of 29.76 and 20.58 mm, respectively. Though QNSE and MYNN are still slightly higher and lower than the other schemes, the area-integrated precipitation shows that over the entire 48-h integration period, there is good agreement among the various schemes in the constant-flux experiments (Fig. 9a).

c. Investigations of the Similarity-Stability Functions

1. Explanation of Similarity-Stability Functions

The relation for HFX is as follows.

$$HFX = -\frac{c_p \rho_o u_* \kappa(\theta_g - \theta_o)}{P_R \psi_h} \quad . \qquad (1)$$

In (1), c_P is the specific heat at constant pressure, ρ_o is the density on the lowest model layer, u_* is the friction velocity, κ is the von Karman constant, θ_g and θ_o are the potential temperature at ground level and on the lowest model layer, P_R is the Prandtl number and Ψ_h is the similarity stability function for heat. The formula for QFX is similar only with θ being replaced by the mixing ratio and Ψ_h being replaced by Ψ_q (the similarity stability function for moisture) in some schemes. Of all of these variables, only Ψ_h and Ψ_q are calculated in the boundary layer scheme. All others are calculated elsewhere. It logically follows that the different HFX and QFX and, consequently, the different precipitation rates, are due to differences in the way Ψ_h and Ψ_q are determined.

Previous research has empirically determined the precise form of these similarity-stability functions as being a function of the stability parameter z/L (Dyer and Hicks 1970; Dyer 1974). The purpose of the similarity-stability functions is to serve as a proxy for turbulence by modifying idealized log profiles for wind, moisture, and θ (for momentum, moisture, and heat, respectively). These log profiles dictate the magnitude of surface exchange coefficients, which are crucial in computing surface fluxes. Therefore, the similarity-stability functions were investigated because they form the basis for the surface fluxes.

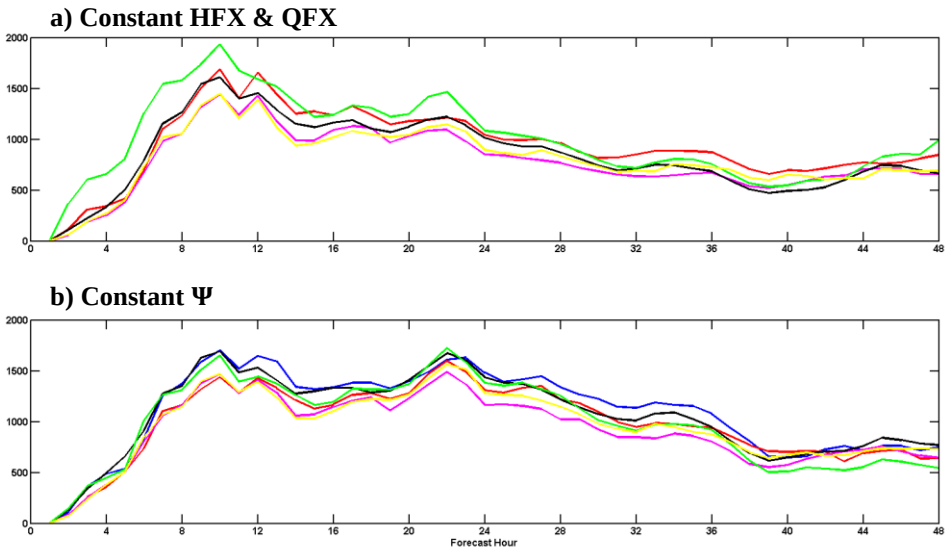

FIG. 9: Area integrated precipitation for the constant-flux experiments (a) and the constant-Ψ experiments (b). When these quantities are held constant in the PBL schemes, it is difficult to distinguish precipitation differences between schemes.

2. Constant Ψ Experiments

In order to test the impact of the similarity-stability functions on precipitation, the over-water values of Ψ are made constant as follows: Ψ_h=8.00, Ψ_m=9.50,and Ψ_q=9.50 . These experiments are referred to as the constant-Ψ experiments. These experiments yield similar results to the constant-flux experiments. Namely, the area-integrated precipitation shows good agreement among the different schemes (Fig. 9b).

4. MODEL VALIDATION

The remaining question that demands attention is which scheme provides the most accurate forecasts. Using the Stage IV analysis (Lin and Mitchell 2005) and Community Collaborative Rain, Hail & Snow Network (CoCoRaHS) observations, 24-hour precipitation forecasts starting at 1200 UTC Dec 10 are compared to control-run model output. Spatially, all schemes place precipitation amounts farther south than both the Stage IV analysis and observations indicate (c.f. Fig. 10a-c,10d). QNSE, MYJ, and MYNN produce total precipitation accumulations consistent with values observed in Section 3a, with QNSE (46.82 mm) producing the most precipitation, MYNN (26.82 mm) producing the least, and MYJ (36.36 mm) producing precipitation consistent with the other schemes not shown (Fig. 10a,b,c).

Three CoCoRaHS sites within the snow band are then compared to point-forecasts of precipitation from the PBL schemes. The sites are: Hamburg, NY, Glenwood, NY, and Perrysburg, NY. Observations at these sites report 24.64 mm at Hamburg, 16.76 mm at Glenwood, and 18.29 mm at Perrysburg. For Hamburg, all schemes forecast at least 50% less precipitation than was observed due to the site being outside of or on the edge of the snow band. For Glenwood and Perrysburg, all schemes forecast more precipitation than was observed. At these locations, MYNN performs best with 21.71 mm at Glenwood and 25.33 mm at Perrysburg. Thus for locations within the snowband, MYNN produced the most accurate forecast. See Table 1 for comparisons of all schemes to CoCoRaHS observations.

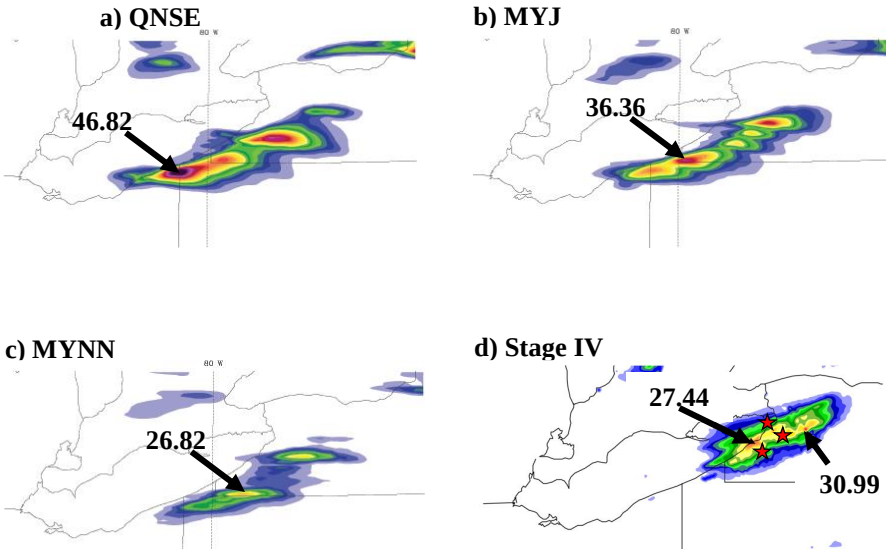

FIG. 10: 24-hour precipitation forecasts (initialized 1200 UTC 10 Dec) for QNSE, MYJ, and MYNN compared with Stage IV analysis. All schemes place precipitation to the south of reality, and MYNN is more accurate than others in capturing the maximum amounts of precipitation. Red stars on (d) indicate locations of point forecasts used. For more information on point-forecast comparisons, see Table 1.

	Hamburg, NY (Erie County)	Glenwood, NY (Erie County)	Perrysburg, NY (Cattaraugus County)
Observation	**24.64 mm**	**16.76 mm**	**18.29 mm**
BouLac	1.79	38.06	44.63
MYJ	1.08	35.12	39.93
MYNN	**3.21**	**21.71**	**25.33**
PX	10.40	33.08	35.38
QNSE	0.70	41.15	40.50
YSU	4.19	24.31	30.48

Table 1: Point forecasts of precipitation (mm) for the three starred locations in Fig. 10 compared to CoCoRaHS observations. All schemes tend to over-forecast precipitation in Glenwood and Perrysburg, NY. Hamburg, NY is under-forecasted due to its location outside on the southern edge of forecasted snow bands. When all three locations are considered, MYNN is the most accurate scheme

5. CONCLUSION

The sensitivity of forecasts of LESN to the choice of boundary-layer parameterization was investigated for a particularly strong LESN event over Lake Erie. A series of control runs reveal that there are significant precipitation differences (as much as 20 mm over a 6-hr period) among the schemes. Trajectory analysis shows that the differences are linked to different degrees of heating, acceleration, and moistening of air as it crosses over Lake Erie. Consideration of the forecast heat and moisture fluxes (HFX and QFX) reveals that those schemes that produce more precipitation have substantially higher fluxes. Tests were performed with the over-water heat and moisture fluxes set to be the same in all schemes. These experiments show much closer agreement in the amount of precipitation.

The equations used to calculate HFX and QFX are functions of several variables that are computed outside of the boundary layer schemes in addition to variables known as the similarity stability functions for heat, momentum, and moisture (Ψ_h, Ψ_m, Ψ_q). These functions provide approximations of the contributions to HFX and QFX via turbulent motions caused by low-level stability gradients. Decreased stability implies stronger turbulence, which, in turn results in larger HFX and QFX. Each scheme uses a different set of assumptions in the calculations of Ψ_h, Ψ_m, and Ψ_q leading to sometimes radically different values of each. To test whether the different Ψ_h, Ψ_m, and Ψ_q were responsible for the different HFX and QFX and, consequently, the different precipitation patterns, a set of experiments were conducted wherein the over-water values of Ψ_h, Ψ_m, and Ψ_q were set to be constant. These experiments show remarkable agreement in the amount of precipitation produced.

Perhaps the more pressing issue with the differing results in the control experiments is not why the differences occur but the knowledge of which scheme is most accurate. To address this, the control experiment results were compared to the stage IV precipitation analyses and CoCoRaHS observations. Location of precipitation was

inconsistent with reality, with precipitation placed south of the actual event. When CoCoRaHS observations at Hamburg, Glenwood, and Perrysburg, NY were considered, it was determined that MYNN produced the most accurate precipitation forecast for this event.

6. ACKNOWLEDGMENTS

This work was prepared by the authors with funding provided by National Science Foundation Grant No. AGS-1062932, and NOAA/Office of Oceanic and Atmospheric Research under NOAA-University of Oklahoma Cooperative Agreement #NA11OAR4320072, U.S. Department of Commerce. The statements, findings, conclusions, and recommendations are those of the author(s) and do not necessarily reflect the views of the National Science Foundation, NOAA, or the U.S. Department of Commerce.

7. REFERENCES

Bougeault, P., and P. Lacarrere, 1989: Parameterization of Orography-Induced Turbulence in a Mesobeta--Scale Model. *Mon. Wea. Rev.*, **117,** 1872-1890.

Dudhia, J., 1989: Numerical study of convection observed during the winter monsson experiment using a mesoscale two-dimensional model. *J. Atmos. Sci.*, **46**, 3077-3107.

Dyer A.J. and Hicks B.B., 1970: Flux-gradient relationships in the constant flux layer. *Quart. J. R. Met. Soc.*, **96**, 715-721.

Dyer A.J., 1974: A review of flux-profile relationships. *Boundary-Layer Meteorology*, **7**, 363-372.

Ek, M., K. E. Mitchell, Y. Lin, E. Rogers, P. Grunmann, V. Koren, G. Gayno, and J. D. Tarpley, 2003: Implementation of the Noah land surface model advances in the National Centers for Environmental Prediction operational mesoscale Eta model. *J. Geophys. Res.*, **108**, 8851, doi: 10.1029/2002JD003296.

Forbes, G. S., and J. H. Merritt, 1984: Mesoscale vorticies over the Great Lakes in wintertime. *Mon. Wea. Rev.*, **112**, 377-381.

Hjelmfelt, M. R., 1992: Orographic Effects in Simulated Lake-Effect Snowstorms over Lake Michigan. *Mon. Wea. Rev.*, **120**, 373-377.

Hong, S., Noh, Y., Dudhia, J., 2006: A New Vertical Diffusion Package with an Explicit Treatment of Entrainment Processes. *Mon. Wea. Rev.* **134**, 2318-2341.

Janjic, Z. I., 2002: Nonsingular implementation of the Mellor-Yemada level 2.5 scheme in the NCEP Meso Model**.** NCEP Office Note 437, 61 pp.

Janjic, Z. I., T. L. Black, M. E. Pyle, H.-Y. Chuang, E. Rogers, G. J. DiMego, 2005: The NECP WRF-NMM core. Preprints, 2005 WRF/MM5 User's Workshop, Boulder, CO, National Center for Atmospheric Research, 2.9. [Available online at http://www.mmm.ucar.edu/wrf/users/workshops/WS2005/presentations/session2/9-Janjic.pdf.]

Kelly, R. D., 1982: A single Doppler radar study of horizontal-roll convection in a lake-effect snow storm. *J. Atmos. Sci*., **39**, 1521-1531.

Laird, N. F., Walsh, J. E., Kristovich, D., 2003: Model Simulations Examining the Relationship of Lake-Effect Morphology to Lake Shape, Wind Direction, and Wind Speed." *Mon. Wea. Rev*., **131,** 2102-2111.

Lin, Y. and K. E. Mitchell, 2005: The NCEP Stage II/IV hourly precipitation analyses: Development and applications. Preprints, 19th Conf. on Hydrology, Amer. Meteor. Soc., San Diego, CA.

Nakanishi, M. and Niino, H., 2004: An Improved Mellor–Yamada Level-3 Model with Condensation Physics: Its Design and Verification. *Boundary-Layer Meteorology,* **112**, 1-31.

Niziol, T. A., 1987: Operational Forecasting of Lake Effect Snowfall in Western and Central New York. *Wea. Forecasting,* **2**, 310-321.

Niziol, T. A., Snyder W. R., Waldstreicher J. S., 1995: Winter Weather Forecasting throughout the Eastern United States. Part IV: Lake Effect Snow. *Wea. Forecasting,* **10**, 61-77.

Peace Jr, R. L., and R. B. Sykes, 1966: Mesoscale study of a lake effects snow storm. *Mon. Wea. Rev.*, **94**, 495-507.

Pleim, J. E., 2007: A Combined Local and Nonlocal Closure Model for the Atmospheric Boundary Layer. Part I: Model Description and Testing. *J. Appl. Meteor. Climatol.,* **46**, 1383-1395.

Reeves, H. D. and D. T. Dawson, 2013: The Dependence of QPF on the Choice of Microphysical Parameterization for Lake-Effect Snowstorms. *J. Appl. Meteor. Climatol.,* **52**, 363-377.

Scott, C. P., P. J. Sousounis, 2001: The utility of additional soundings for forecasting lake-effect snow in the Great Lakes. *Wea. Forecasting*, **16**, 448-462.

Shi, J. J., W.-K. Tao, T. Matsui, R. Cifelli, A. Hou, S. Lang, A. Tokay, N.-Y. Wang, C. Peters-Lidard, B. Skofronick-Jackson, S. Rutledge, and W. Peterson, 2010: WRF simulations of the 20-22 January 2007 snow events over eastern Canada: Comparison with in situ and satellite observations. *J. Appl. Meteor. Climatol.*, **49**, 2246-2266.

Sukoriansky, S., Galperin, B., Perov, V., 2006: A quasi-normal scale elimination model of turbulence and its application to stably stratified flows. *Nonlin. Processes Geophys.* **13**, 9-22.

Theeuwes, N. E., G. J. Steeneveld, F. Krikken, and A. A. M. Holtslag, 2010: Mesoscale modeling of lake effect snow over Lake Erie - sensitivity to convection, microphysics and the water temperature. *Adv. Sci. Res.*, **4**, 15-22.

Thompson, G., R. M. Rasmussen, and K. Manning, 2004: Explicit forecasts of winter precipitation using an improved bulk microphysics scheme. Part I: Description and sensitivity analysis. *Mon. Wea. Rev.*, **132**, 519-542.

Vavrus, S. M. Noraro, A. Zarrin, 2013: The role of ice cover in heavy lake-effect snowstorms over the Great Lakes basin as simulated by RegCM4. *Mon. Wea. Rev.*, **141**, 148-165.

Wright, D. M., D. J. Posselt, and A. L. Steiner, 2013: Sensitivity of lake-effect snowfall to lake ice cover and temperature in the Great Lakes region. *Mon. Wea. Rev.*, **141**, 670-689.

Zhao, L., J. Jin, S.-Y. Wang, M. B. Ek, 2012: Integration of remote-sensing data with WRF to improve lake-effect precipitation simulations over the Great Lakes region. *J. Geophys. Res.*, **117**, 1-12.